Knighton James (Orcid ID: 0000-0002-4162-996X)

Kuppel Sylvain (Orcid ID: 0000-0003-3632-2100)

Using Isotopes to Incorporate Tree Water Storage and Mixing Dynamics into a Distributed Ecohydrologic Modelling Framework

James Knighton[1,2], Sylvain Kuppel[3,4,5], Aaron Smith[6], Chris Soulsby[5,6], Matthias Sprenger[7,8], and Doerthe Tetzlaff[6,9]

[1] Department of Biological and Environmental Engineering, Cornell University, NY, USA

[2] The National Socio-Environmental Synthesis Center, Annapolis, MD, USA

[3] IPGP, CNRS-UMR 7154, Univ. Paris Diderot, USPC, Paris 75231, France.

[4] Irstea, UR RiverLy, Centre de Lyon-Villeurbanne, 69625 Villeurbanne, France.

[5] Northern Rivers Institute, University of Aberdeen, Aberdeen, AB24 3UF, United Kingdom.

[6] Leibniz-Institute of Freshwater Ecology and Inland Fisheries (IGB), Berlin, 12587, Germany

[7] Institute of Environmental Assessment and Water Research (IDEA-CSIC), Barcelona, Spain

[8] Department of Forestry and Environmental Resources, North Carolina State University, Raleigh, NC , USA

[9] Department of Geography, Humboldt University Berlin, Berlin, 10099, Germany.

[1] Corresponding Author: jok8@cornell.edu; Phone: 1-215-317-0980; Mailing Address: Dept. of Biological and Environmental Engineering, Cornell University, Ithaca, NY 14853-5701
2 sylvain.kuppel@irstea.fr
3 mspreng@ncsu.edu
4 smith@igb-berlin.de
5 c.soulsby@abdn.ac.uk
6 d.tetzlaff@igb-berlin.de

Abstract: Root Water Uptake (RWU) by vegetation influences the partitioning of water between transpiration, evaporation, percolation, and surface runoff. Measurements of stable isotopes in water have facilitated estimates of the depth distribution of RWU for various tree species through methodologies based on End Member Mixing Analysis (EMMA). EMMA often assumes that the isotopic composition of tree-stored xylem water (δ_{XYLEM}) is representative of the isotopic composition of RWU (δ_{RWU}). We tested this assumption within the framework of EcH$_2$O-iso, a process-based distributed tracer-aided ecohydrologic model, applied to a small temperate catchment with a vegetation cover of coniferous Eastern Hemlock (*Tsuga canadensis*) and deciduous American Beech (*Fagus grandifolia*). We simulated three scenarios for tree water storage and mixing: 1) zero storage (ZS), 2) storage with a well-mixed reservoir (WM) and 3) storage with piston flow (PF). Simulating tree storage (WM and PF) improved the fit to δ_{XYLEM} observations over ZS in the summer and fall seasons, and substantially altered calibrated RWU depths and stomatal conductance. Our results suggest that there are likely to be advantages to considering tree storage and internal mixing when attempting to interpret δ_{XYLEM} in the estimation of RWU depths and critical zone water residence times, particularly during periods of low transpiration. Improved representations of tree water dynamics could yield more accurate ecohydrologic and earth system model representations of the critical zone.

1. Introduction

The rooting zone is a highly dynamic part of the critical zone which strongly influences the fate and transport of terrestrial water and its dissolved chemical constituents. Rooting zone water content controls saturation-excess partitioning between surface runoff and infiltration, and further partitioning of the infiltrated water between groundwater recharge and local atmospheric return through soil evaporation and transpiration. On land, transpiration by green plants is often the dominant flux of water return to the atmosphere (Schlesinger & Jasechko, 2014; Good et al., 2015), providing a critical control on stored water in the rooting zone. Despite the importance of plant roots in mediating soil water and dissolved nutrient dynamics, the study of root and soil water interactions remains a developing field with many open questions (Penna et al., 2019; Brantley et al., 2018; Berry et al., 2017).

Emerging methods using stable isotopes in water (^{2}H and ^{18}O) have led to insights into the age distributions of soil water percolate and plant Root Water Uptake (RWU) (e.g. Sprenger et al., 2019, 2018; Evaristo et al., 2019; Benettin et al., 2019; Smith et al In Review; Knighton et al 2019a). Recent studies have employed stable isotopes and variations of the End Member Mixing Analysis (EMMA) methodology to estimate the proportional contribution of different subsurface water sources to RWU. EMMA is a statistical approach to estimating the relative contribution of multiple sources (i.e. subsurface waters) to an integrated mixture of these sources (i.e. tree-stored water) which can be inferred from measured isotopic compositions in water. Studies investigating RWU depths have been motivated by a desire to understand the prevalence of ecohydrologic separation (Evaristo et al., 2019), climate adaptation strategies of plants (Brinkman et al., 2019; Evaristo & McDonnell, 2017; Barbeta & Peñulas, 2017), RWU competition among native and invasive species (De Deurwaerder et al., 2018), optimal revegetation schemes for modified landscapes (Wang et al., 2017; 2019), hydroclimatic extremes following anticipated tree species succession (Knighton et al 2019b), and to better resolve the functional traits of trees in land surface models (Matheny et al., 2017).

Rothfuss & Javaux (2017), Barbeta et al. (2018), Penna et al. (2018), De Deurwaerder et al (2019), and Wang et al. (2019) highlighted conceptual limitations of the EMMA approach in that we must assume measured soil water isotopic compositions are representative of available water sources at the time of RWU. Goldsmith et al. (2019) demonstrated that spatial and temporal variability in soil water can influence RWU depth estimates. Further, EMMA requires the assumption that the measured isotopic compositions of xylem waters (δ_{XYLEM}) are representative of the RWU isotopic composition (δ_{RWU}), suggesting that water storage and mixing within trees is negligible. However, experimental studies of residence times within trees challenge this assumption (Köcher et al., 2013; Čermák et al., 2007; Urban et al., 2015; Meinzer et al., 2006).

Internal storage of mobile water within trees is a biological adaptation that reduces water stress during periods of reduced soil water availability and RWU (e.g. Sanchez-Costa et al., 2015). Capacitive discharge (forced transpiration from tree-stored water) provides a biological resilience against embolism (Scholz et al., 2011). Tree-stored water has been shown to contribute up to 20% of daily transpiration during the peak growing season within Douglas fir (*Pseudotsuga menziesii*) in a Mediterranean climate (Phillips et al., 2003; Čermák et al., 2007), the genera *Fagus*, *Tilia*, *Carpinus*, *Fraxinus* and *Acer* within a temperate climate (Kocher et al., 2013), and Scots Pine (*Pinus sylvestris*) in a temperate maritime climate (Urban et al.,

2015). Within time periods of reduced plant growth and atmospheric water demand, transpiration from Douglas fir can be sourced solely from tree-stored water for up to one week (Čermák et al., 2007). Hao et al. (2013) observed a steady decrease in the Volumetric Water Content (VWC) of the main stems of *Betula papyrifera* trees, measured by frequency domain reflectometry sensors throughout the growing season. Urban et al. (2015) estimated the xylem storage volume of a Scots Pine stand in Belgium to be approximately 9 mm (rainfall equivalent), a potentially significant reservoir for mixing during periods of low transpiration. Together, these studies suggest that the mean residence time of water within trees (i.e. the mean age of all water stored within the tree) could induce a significant time lag between the isotopic composition of stored xylem water (δ_{XYLEM}), soil water (δ_{SOILS}), and gross precipitation (δ_{GP}).

The advent of process-based isotope-aided hydrologic models (e.g. Kuppel et al., 2018a; Knighton et al., 2017; Smith et al., 2016; Haverd & Kuntz, 2010; Yoshimura et al., 2006; Braud et al., 2005) can help relax our reliance on the assumption of time invariance for δ_{SOILS} and δ_{RWU}; however, a lack of empirical studies has prevented the process of storage and mixing within trees from being resolved in most current generation model structures. Wen et al (2016) demonstrated that the isotopic composition of *Zea mays* xylem deviated from that of transpired water during periods of low transpiration. Yoshimura et al (2006) tracked the isotopic composition of soils, as well as trunk- and leaf-water within trees. Their modeling approach suggested the isotopic signature of stem water could deviate substantially from subsurface waters.

Time lags between δ_{GP} and δ_{XYLEM} have been observed across catchments with varied geologies and climates (e.g. Allen et al., 2019; Knighton et al 2019a; Smith et al In Review; Brinkman et al., 2018), which each study attributed to the residence time within catchment soils prior to RWU. These studies incorporated the open assumption that δ_{XYLEM} reflects the composition of δ_{RWU} as a reasonable approximation at the catchment-scale during the growing season. This implies that tree storage and within-tree mixing dynamics are negligible, assumptions which possibly limit the interpretation of δ_{XYLEM} observations (Penna et al., 2018). While water residence within soils is likely an important mechanism for increasing the age of critical zone water (e.g., Sprenger et al., 2018; Kuppel et al., 2018a; Chitra-Tarak et al., 2018; Knighton et al., 2019a), transient storage and mixing dynamics within trees possibly causes the age distribution of tree stored water to deviate from that of RWU. Brooks et al. (2010), Treydte et al. (2014), McCutcheon et al. (2017) and Knighton et al. (2019a,b) hypothesized that δ_{XYLEM} measurements made during the dormant season may be more representative of δ_{RWU} from waters infiltrated during an extended antecedent period prior to vegetation sampling due to reduced or ceased dormant season transpiration.

Further, we know relatively little about the degree of mixing between older tree-stored water and new RWU, and how this uncertainty influences our interpretation of δ_{XYLEM} (Berry et al., 2017). Most tree-stored water is retained in the heartwood and is hydraulically separated from mobile sapwood (e.g. Zimmerman, 1971; Kravka et al 1999; Urban et al., 2015), leaving only a portion of stored water available for mixing with RWU. Meinzer et al. (2006) studied sap flux dynamics of two conifer species through injection of ^{2}H labeled water. Mean tracer residence times exceeded upper crown arrival times by approximately 200% (Meinzer et al., 2006), suggesting internal recycling or diffusion. Matheny et al. (2015) hypothesized that deciduous Oak trees (*Quercus sp.*) may access older xylem water during periods of soil water limitation. Wen et al (2016) observed minimal separation between water within *Zea mays* and

transpired waters during peak daily transpiration suggesting a well mixed storage. De Deurwaerder et al (2019) observed stem water isotopic variations along the lengths of six deciduous tree species in French Guiana and northwestern China, implying that mobile tree stored water is not necessarily well-mixed. We therefore propose that 1) complete mixing, that is transpired water draws uniformly from all tree-stored water independent of water age, and 2) piston flow, where transpired water is sourced from the oldest tree-stored water, could each represent a working hypothesis for modelling the transport of tree-stored water from root to leaf. We select these two concepts as the extreme bounds on internal tree water mixing at the plot-scale.

To test these working hypotheses, we present a novel modelling-based approach for the explicit simulation of tree water storage and mixing, using the distributed isotope-enabled ecohydrologic modeling framework of Maneta et al. (2013) and Kuppel et al. (2018a). These modeling advances are proposed as a way of addressing the following research questions:

- Does explicit simulation of tree water storage improve model calibration to δ_{XYLEM} observations?
- Are tree-stored water dynamics better approximated through simulating a uniform selection of stored water by transpiration (i.e., immediate, full mixing of RWU), or a preferential selection of the oldest stored water (i.e. piston flow)?
- Are tree-storage residence times of similar magnitude to soil water residence times?

We evaluate these questions with a study of a small temperate catchment in central New York, US, densely vegetated with both the coniferous Eastern Hemlock (*Tsuga canadensis*; hemlock) and deciduous American Beech (*Fagus grandifolia*; beech). Developing explicit representations of tree-storage and mixing within isotope-aided hydrologic models could assist interpretation of xylem isotopic compositions, therefore providing more reliable estimates of vegetation RWU depths and critical zone residence times.

2. Methodology

2.1 Site Description

The modelling experiment was based on a 1.2 km^2 catchment in central NY, US (42.42°, -76.32°) in a temperate climate region. The catchment receives approximately 1,000 mm of precipitation annually, with approximately 60% of annual precipitation occurring during the growing season (mean monthly air temperatures greater than 10°C from April through November). Annual evapotranspiration in this catchment is approximately 500 mm^{1}year^{-1} (Knighton et al 2019a). Freezing air temperatures persist from December through March, leading to the establishment of a snowpack throughout the winter season (approximately 20% of annual precipitation).

Catchment soils were characterized as Cambisols. Sand, silt, and clay compositions were estimated with the hydrometer method (Gee & Bauder, 1986). Organic content of soils was estimated as the mass difference of samples oven-dried and then heated to 550°C for 3 hours. Hilltop soils are composed of a 5 cm organic layer underlain by silt loam. Riparian soils are the same texture, but with no organic surface layer. Soil textures of the upper 50 cm are uniform with increasing gravel contents by mass ranging from 0 - 22% at the surface to 38 - 71% at 30 cm. Catchment soil bulk densities range from 1.3 to 1.58 g^{1}cm^{-3} (NRCS, 2019). The catchment is underlain by highly weathered siltstone bedrock at an average depth of 50 cm and a confining

layer between 1 and 1.5 m (NRCS, 2019; Schneiderman et al., 2007). The median catchment slope is 20°.

Catchment tree cover is composed primarily of second-generation regrowth (stand age approximately 60 years) deciduous American Beech (beech) and coniferous Eastern Hemlock (hemlock) (Fig. 1), though other deciduous species exist at lower densities (Knighton et al 2019a). Within the mixed hemlock /beech region, hemlock and beech densities are 0.031 m^{-2} and 0.012 m^{-2} respectively. All beech and hemlock trees were respectively unaffected by hemlock wooly adelgid infestation and beech bark disease at the time of sampling. The deciduous leaf-on season extends on average from approximately April 1st through November 1st, though beech typically holds leaves past the growing season for an 11-month period. The rooting depth profile of beech is predominantly shallow, where Yanai et al. (2008) found approximately 80% of beech fine roots exist within the upper 30 cm. Hemlock maximum rooting depth typically extends to the regional average water table depth, though Meinzer et al. (2013) demonstrated that hemlock sapflux through the growing season was strongly correlated with the soil water content of the upper 50 cm. The peak growing season leaf area indices (LAIs) of hemlock and *Fagus sp.* vary from approximately 6 to 8 (m^{2}m^{-2}) (Naithani et al., 2013; Leuschner et al., 2006; Bartelink, 1997). Canopy interception for hemlock and beech is approximately 15% (Guswa & Spence, 2011) and 18% (Staelens et al., 2006), respectively, of gross precipitation for rainfall events exceeding 10 mm.

2.2 Field Collections and Lab Analysis

We measured daily gross precipitation with a 200-mm diameter tipping bucket rain gage (TR-525-S-U, Texas Electronic; precision = 0.2 mm and accuracy = +/- 3%), in a clearing approximately 1 km from the catchment outlet (Fig. 1). Daily catchment stream discharge was derived from measurements made with a HOBO pressure transducer. Daily maximum and minimum air temperatures were measured with a HOBO sensor near the catchment outlet. We measured weekly gross precipitation isotopic composition, δ_{GP}, near the rain gage. Weekly instantaneous stream water isotopic composition, δ_{stream}, was measured at the pressure transducer. We measured Snowpack Water Equivalent (SWE) and snowpack isotopic composition (δ_{SWE}) as a point measurement near the catchment outlet at a weekly interval during the cool season (Fig. 1). Isotopic measurements are reported with respect to the Vienna Standard Mean Ocean Water 2 (VSMOW2).

At six locations along a hillslope (Table 1), we measured weekly soil volumetric water content (VWC) and bulk δ_{SOILS} at a depth of 5 to 10 cm. Shallow soil (top 12 cm) VWC measurements were made weekly with a 12 cm long Time Domain Reflectivity (TDR) probe (CS658, Campbell Scientific; resolution = 0.05%, accuracy = 3%). Soil isotopic depth profiles were collected seasonally (August 13th, 2017, November 12th, 2017, June 5th, 2018) at 5 cm increments to a depth of 50 cm or until weathered bedrock was encountered. For each sample, approximately 100 mL of soil were collected at each location each week from January 2017 to January 2018 with a hand pick and immediately placed into a sealed jar.

We estimated the seasonal isotopic composition of xylem water with a total of 99 beech and 108 hemlock stems. Across each of three seasons, we sampled 69 individual trees of (33 beech and 36 hemlock). These samples were collected uniformly across the six sampling locations (Fig. 1; 12 samples at each location, except site 2 where only 3 beech samples were collected). Plant stems were sampled on 1) August 13th, 2017, during a period of particularly dry shallow

soil conditions at upland locations within the growing season where trees may be expected to supplement RWU from deeper layers, 2) November 12th, 2017 several days after a soil water recharge event by isotopically depleted precipitation, and 3) June 5th, 2018 four weeks following the bud burst of beech and after the last spring snowmelt. Sampled trees had a minimum and maximum DAB of 5 and 30 cm respectively. All branches were sampled at a height of approximately 1.5 m. Stem samples were clipped to approximately 5 cm length (1 cm diameter) from branches near the trunk, a minimum of 1 m away from transpiring leaves. Clipped ends of the stems were covered in parafilm and placed into sealed jars immediately.

Collected soils and stems were stored frozen prior to cryogenic vacuum extraction of water. Extractions were run for a minimum of 180 minutes, at a temperature differential of 280°C, at a maximum pressure of 10 kPa in order to minimize errors (Orlowski et al., 2016; 2018). Soil and plant xylem waters were analyzed with an off-axis integrated cavity output spectrometer (OA-ICOS; IWA-35EP, Los Gatos Research, Mountain View, CA, USA) coupled with an autosampler (LC PAL, CTC Analytics AG, Zwingen, Switzerland) for liquid sample injections (precision of 0.5‰ for δ^2H and 0.1‰ for $\delta^{18}O$). Isotopic data was calibrated to the VSMOW2 reference scale with three water standards covering the isotopic range of natural water. Gross precipitation, throughfall, stream water, and SWE samples were analyzed on a Thermo Delta V isotope ratio mass spectrometer interfaced to a Gas Bench II (precision of 0.5‰ for δ^2H and 0.24‰ for $\delta^{18}O$). The depth variability of soil $\delta^{18}O$ is shown in supplemental Figure S1.

2.3 Model Description

We utilized EcH$_2$O-iso, a fully distributed process-based hydrologic model capable of simulating plant growth and dynamics of stable isotopes (^2H and ^{18}O) in water (Maneta et al., 2013; Kuppel et al., 2018a, b; Douinot et al., 2019). The modelled domain was constructed on a 10×10 m^2 horizontal grid. The hydrologic and plant dynamic computational time step was 1 day in all simulations. Land cover in the catchment was defined with two vegetation classes respectively corresponding to beech and hemlock; part of the catchment is considering to be exclusively covered by beech, and the remaining area by a mixture of hemlock and beech with initial densities of 0.031 m^{-2} and 0.012 m^{-2} respectively (Fig. 1). All soil and tree sampling sites were located within the area of mixed hemlock and beech. Further details of the EcH$_2$O-iso representation of soils, the rooting distribution, and model parameters are presented in the supplemental material.

We utilized three model structures for the representation of the xylem isotopic composition:

- Zero storage case (ZS): We assumed storage (and thus mixing) within the hemlock and beech trees is negligible. Field measurements were compared directly to the simulated RWU isotopic composition based on the EcH$_2$O-iso conceptualization of rooting distribution and soil water isotopic composition.
- Well-mixed storage case (WM): We assumed storage within hemlock and beech trees cannot be neglected. We introduce two new parameters (*Tree$_V$* defined for both species; representing the reservoir sizes as a length) provided by hemlock and beech at the tree and soil sampling locations. We further assumed that the age of transpiration losses is an average across tree-stored water.
- Piston flow case (PF): Same as WM; however, we assumed that transpiration within trees preferentially uses oldest stored water. This case represents piston flow within the hemlock and beech trees.

2.4 Model Calibration

EcH2O-iso calibration was performed against both catchment-scale observations (stream discharge, δ_{STREAM}) as well as plot scale measurements of SWE, shallow soil VWC, and stable isotopic compositions (^{18}O) of shallow bulk soil water and xylem water of hemlock and beech (Table 2). Simulated δ_{XYLEM} was calibrated against both the residuals of the d-excess as well as the residuals of the observed and simulated projections onto the Global Meteoric Water Line (GMWL), termed MWL. Metrics for plant xylem calibration were chosen such that each measurement was orthogonal. Computation of MWL proceeded as follows: We first translated the GMWL and all isotopic observations such that the translated GMWL passes through the origin, $\delta^2 H^O = \delta^2 H - 10‰$. We then defined the unit vector of the translated GMWL, w, such that $w = \frac{[\delta^2 H^O \quad \delta^{18}O]}{\|[\delta^2 H^O \quad \delta^{18}O]\|}$. We computed the projection matrix, P, such that $\frac{ww^T}{\|w\|^2}$, where w^T is the transpose of the vector w. We then calculated the projection of all observations and simulated isotopic values, $x = [\delta^2 H^O \quad \delta^{18}O]$, onto the translated GMWL, x^P, such that $x^P = Px$. MWL was then calculated as the distance between x_{obs}^P and x^P. The computation of MWL is shown graphically in the supplemental material (Fig. S2).

We calibrated to soils only at sampling locations 2 and 5 to constrain the model with a topographically dry and wet location (Fig. 1, Table 2). Soil predictions at sites 1, 3, 4, and 6 were used for validation. As our research focus was centered on model representations of vegetation, we calibrated the model against plant observations made at all sampling locations.

We simultaneously constrained EcH2O-iso parameters (Table 3) to all measurements utilizing a Markov Chain Monte Carlo approach with the Metropolis Hastings sampler and Generalized Likelihood (GL) function of Schoups & Vrugt (2010). We ran 20,000 model parameter evaluations for each of the three proposed model structures. The total number of parameter evaluations was determined by visually identifying stability in the GL function value. The first 2,000 model parameter evaluations were discarded as the "burn-in" period. This approach allows multiple datasets to be used for calibration, where each dataset is weighted based on the magnitude of the residuals and record length (Schoups & Vrugt, 2010). The GL function provides an objective measure of the distance between simulation and observed time series while controlling for autocorrelation, heteroscedasticity, non-normality of the resulting distribution of residuals, and record length. We simultaneously fit hydrologic and plant dynamic model parameters and a statistical model for residuals (Schoups & Vrugt, 2010). Model calibration parameters and feasible ranges were selected based on previous calibration efforts involving EcH2O (Kuppel et al., 2018b) and EcH2O-iso (Kuppel et al., 2018a; Douinot et al., 2019). In contrast to Kuppel et al. (2018a,b) we calibrated species specific RWU profiles for hemlock and beech through K_{ROOT}. The upper limit of $Tree_V$ (Table 3) for each species was set to an arbitrarily large value (150 mm) to prevent *a priori* numerical restriction of a model parameter of which we have limited prior knowledge. This calibration methodology was repeated for the ZS, WM, and PF model structures. Finally, we visually compared δ_{XYLEM} simulations in the dual-isotope space.

Accurate simulation of both plot-scale and catchment-scale processes presents an inherent challenge for hydrologic models (Clark et al., 2015). The supplemental material presents an analysis of MCMC parameter evaluations for the WM case (Fig. S3), and a sensitivity analysis

to examine calibration tradeoffs between catchment-scale and plot-scale measurements (Fig. S7).

2.5 Water Ages, RWU Transit Times & Tree Storage Residence Times

We estimated transit times of RWU and the mean residence times within hemlock and beech trees to determine if residence within trees was a significant contribution to total critical zone water residence times. Within the EcH$_2$O-iso model, gross precipitation ages are zero. The ages of water in storage (i.e., residence times) are increased by one day at the end of each simulated daily time step (e.g. snowpack, soils, groundwater). All these compartments are simulated as fully mixed and representative of the bulk δ_{SOILS}. As a result, EcH$_2$O-iso currently only simulates mean residence times in each storage compartment. In particular, transit times of RWU are directly derived from the water residence times in all soil layers, weighted proportionally to each layer's contribution. Further details on EcH$_2$O-iso water age tracking is presented in Kuppel et al. (2018a). Residence times presented are the median estimates of all accepted posterior model parameterizations.

Residence times within trees are computed with respect to the storage of mobile waters within trees, neglecting any hydraulically immobile water stored in heartwoods. This mobile water storage volume is assumed to exist as a constant volume $Tree_V$ determined through calibration (Table 3). The mean residence time within tree storage is computed as the mobile water storage volume provided by trees (the parameter $Tree_V$, Table 3) divided by the simulated rate of leaf transpiration flux. Our methodology assumes that only one outflux of water from trees (i.e. leaf transpiration) occurs. This approach also assumes that the mobile water storage volume available within trees is constant, an assumption that is challenged by several existing studies (Matheny et al., 2015; Čermák et al., 2007; Hao et al., 2013). This simplifying assumption was chosen to limit model dimensionality. This approach to estimating the mean residence times applies to both the WM and PF structures.

3. Results

3.1 Model Calibration Results Incorporating Storage and Mixing Dynamics within Trees

3.1.1 Calibration Metrics

Observed precipitation and discharge time series are presented in Fig. 2a. The EcH$_2$O-iso simulated discharge and stream δ^{18}O in all model structures (ZS, WM, and PF) provided a reasonable approximation of the observations (Fig. S4). Modelled daily stream discharge Mean Absolute Error (MAE) for ZS, WM and PF was 0.02 m^{3}s^{-1}. Percent bias for ZS, WM, and PF was -20.32%, -22.18%, and -23.08% respectively. All three model structures overestimated the isotopic enrichment of stream water and underestimated the volume of discharge.

We present calibration results of the ZS model to plot-scale measurements of shallow soil (top 10 cm) VWC and δ_{SOILS} (Fig. 2b). Calibration results of the WM and PF models (presented in the supplemental material) were very similar to ZS. All models performed adequately for the soil water content (RMSE range = [0.048 m^{3}m^{-3}, 0.063 m^{3}m^{-3}]) and bulk δ_{SOILS} (RMSE range = [2.19 ‰, 3.34 ‰]) at all locations (Fig. 2b, S5, S6). The seasonality of bulk δ_{SOILS} was reproduced well across all locations with enriched soil water in the summer and more depleted water in the cool season. EcH$_2$O-iso simulates immediate, full mixing in each soil compartment as water percolates, i.e. draws uniformly from all water ages (Kuppel et al., 2018a). This

approximation resulted in a slight overestimation δ_{SOILS} during the warm season across all sites (Fig. 2b). As demonstrated in the supplemental material (Fig. S7a) the EcH$_2$O-iso model parameterization achieved an improved representation of soils and plant xylem at the expense of catchment scale fluxes (stream discharge).

We present the residuals between the centroids of simulated and observed hemlock and beech δ_{XYLEM} for the d-excess and MWL in Table 4. For beech, all three model cases (ZS, WM, and PF) provided reasonable approximations of δ_{XYLEM} composition during the summer and spring at all sites (Table 4; Fig. 3). For hemlock, WM and PF provided stronger approximations of δ_{XYLEM} during the growing season, where PF provided the most consistent minimization of residuals (Table 4; Fig. 4). ZS performed substantially worse for hemlock across all seasons.

At the onset of the fall and the start of rewetting, soil water was rapidly replenished by precipitation as plant transpiration was reduced. This cool season precipitation rapidly depleted δ_{SOILS} (Figures 2, S3 and S4). ZS, which assumes tree stored water can be approximated by same day RWU, resulted in no estimate of δ_{XYLEM} during the fall for beech as RWU had ceased (Fig. 3, S7). Similarly, the ZS model provided a poor estimate of the fall δ_{XYLEM} observations for hemlock (Fig. 4, S7). As a coniferous tree species, transpiration in hemlock was simulated during the fall stem collection; however, the δ_{RWU}, which draws on the soil water rewetted by depleted precipitation, was substantially more depleted than δ_{XYLEM} sampled in the fall (Fig. 4).

The WM and PF models, which simulate a water storage reservoir within the tree, provided closer agreement between simulated and observed fall δ_{XYLEM} for both hemlock and beech (Table 4; Fig. 3 and 4). For hemlock, the assumption of PF provided the most consistent minimization of residuals, except for MWL in the spring season (Table 4). In the case of beech trees the most appropriate model approximation of tree dynamics was less clear with as there was no consistently strong model structure (Table 4). In spring, all three models performed approximately evenly for beech. During fall, both WM and PF, performed similarly, with a slightly better performance by PF. In spring, both WM and ZS models performed well at reproducing different aspects of beech δ_{XYLEM} in the dual isotope space (Table 4, Fig. 3).

3.1.2 Influence of Tree Dynamics on Hydrologic and Plant Parameters

The marginal posterior distributions of EcH$_2$O-iso hydrologic parameters for the ZS, WM, and PF cases are presented in Fig. 5 (all parameter evaluations for WM case presented in Fig. S3). Posterior distributions of hydrologic model parameters, largely controlling snowmelt and runoff were consistent between each case. There were slight differences in parameters that influenced soil water retention and movement ψ_{AE} and $KvKh$ (Fig. 5). We note that the differences in structural assumptions concerning tree-dynamics had a negligible influence on catchment-scale simulation of discharge and δ_{STREAM} (Fig. S4).

The posterior distributions of the EcH$_2$O-iso plant dynamics parameter ψ_D was relatively stable across the ZS, WM, and PF model structures (Fig. 6). Estimates of the optimal growth temperature (T_{OPT}), maximal stomatal conductance (g_{Smax}), maximum canopy water storage (CWS_{max}), and the light extinction coefficient (K_{BEERS}) varied across the model structures. For the ZS, WM, and PF cases the root water uptake depth distribution parameter, K_{ROOT}, suggested substantial differences between hemlock and beech. The WM assumption led to a K_{ROOT} value indicating shallower soil water uptake by beech, whereas the PF case indicated deeper RWU.

For both the WM and PF model structures, $Tree_V$ differed by species with hemlock possibly providing a larger internal reservoir than beech (Fig. 6). The estimated mobile water storage volume within hemlock trees was fairly consistent between each model structure, around 75 mm (rainfall equivalent depth). Estimated storage provided by beech trees differed between WM (~25 mm) and PF (~50mm) (Fig. 6). Calibrated $Tree_V$ values for the coniferous hemlock were roughly an order of magnitude greater than the xylem-storage estimated for Scots Pine by Urban et al. (2015).

3.3 Influence of Internal Tree Mixing Dynamics on Critical Zone Residence Times

We utilized the median of accepted model simulations to estimate the mean 2017 growing season soil and tree storage residence times for hemlock and beech under the assumptions of WM and PF (Fig. 7). Both model structures produced similar mean transit times of RWU and mean residence times within hemlock and beech. The residence times of soil waters taken up by plant roots varied from approximately 50 to 250 days throughout the growing season, with these water ages increasing with topographic wetness as soil water storage and mixing increases (Fig. 7). The peak growing season (June – August) tree storage residence times for hemlock varied from 20 to 100 days, and 5 to 50 days for beech in both the WM and PF models. Simulated residence times increased from September through March at all sampling locations as a result of decreased transpiration rates.

4. Discussion

4.1 Model Calibration Incorporating Storage and Mixing Dynamics within Trees

This analysis was centered on 99 and 108 δ_{XYLEM} samples of beech and hemlock, respectively. Observations provided a strong spatial coverage across a gradient of TWI, but only at three points in time across the growing season. Previous studies have demonstrated that variations in RWU and transpiration can occur over several hours (e.g., Nehemy et al 2019; Volkmann et al., 2016; Yoshimura et al., 2006). Though our analysis formally acknowledges uncertainty in parameter estimation (Figures 3, 4, 5, and 6), our results and the following discussion are predicated on the structure of EcH_2O-iso and our representations of tree-water storage as adequate abstractions of relevant ecohydrological processes. Future research should more critically evaluate RWU and mixing with more frequent measurements of δ_{XYLEM} through time, and explore the possibility of time varying ecohydrologic parameterizations or more physically-based representations of RWU demand that adequately describe temporal variations in RWU (e.g. Mackay et al 2020).

Simulation of tree reservoir volumes (in the WM and PF models) produced a better fit to observations of δ_{XYLEM} than ZS, particularly in the fall season for both hemlock and beech, as the trees entered dormancy and the catchment soils were recharged with depleted precipitation (Table 4). The WM and PF assumptions both provided reasonable estimates of δ_{XYLEM} within both hemlock and beech across all seasons, though PF more consistently minimized residuals for hemlock (Table 4). Previous observations that the mean residence time of a conservative tracer exceeded the root to leaf arrival time within trees (Meinzer et al., 2006) suggest that perfect PF is not occurring within the trees. Deciduous trees possibly mobilize younger xylem during periods of soil water availability and older xylem during soil water limitation (Matheny et al., 2015). These studies, while refuting perfect PF, also do not well describe WM. Our research suggested that for hemlock the more appropriate representation of internal mixing was

PF. In reality, internal mixing and diffusion likely occur, resulting in storage dynamics characterized somewhere between the WM and PF assumptions.

Within beech trees the most appropriate assumption for tree storage dynamics was less clear, given observations of δ_{XYLEM} in the spring and summer. Posterior distributions of tree storage under the WM and PF assumptions suggested that the reservoir provided by beech trees was substantially less than that of hemlock (Fig. 6). If beech tree xylem storage is in fact lower than hemlock, we would anticipate reduced sensitivity to the representation of mixing dynamics within beech relative to hemlock, possibly explaining the lack of a clearly optimal model structure for beech (Table 4, Fig. 6). It is possible that the reproduction of δ_{XYLEM} within a hydrologic modeling framework is a consideration that should be reserved for the simulation of trees with large dynamic-storage capacities. Dynamic storage and mixing, particularly within deciduous trees (Matheny et al., 2015), is likely more complex than the model structures presented here. We hypothesize that these characteristics will vary by species and stand age. Alternate model structures, such as those accounting for back diffusion of enriched leaf water (Yoshimura et al., 2006) should be explored.

4.2 Implications for Estimating RWU Depth Distributions

We obtained significantly different RWU depth demand profiles (as represented by the K_{ROOT} parameter) for beech when the representation of tree storage and mixing was changed between ZS, WM, and PF (Fig. 6). This result calls into question the EMMA approach for estimating the sources of RWU, as simulated δ_{XYLEM} of both hemlock and beech were influenced not only by K_{ROOT}, but also by the simulated tree storage volumes (Fig. 6), and time lags between δ_{XYLEM} and δ_{RWU}. In the absence of additional data to constrain internal plant hydraulics, measurements of δ_{XYLEM} and δ_{SOILS} alone may not provide meaningful information on RWU depth profiles. We may therefore improve our understanding of soil-root interactions through modelling approaches constrained by multiple hydrologic and meteorological observations (e.g. Knighton et al., 2020; Kuppel et al., 2018b), by more detailed biological measurements such as LAI, transpiration rates, and biomass (Douinot et al., 2019) and photosynthesis rates (Peaucelle et al., 2019). Insights into RWU could be gained through direct observation of subsurface flows (e.g. Jackisch et al., 2017) and prior knowledge of the functional traits of tree roots (Comas et al., 2009; Kattge et al., 2011). There are likely to be advantages to considering tree storage and mixing when attempting to interpret δ_{XYLEM}, particularly during periods of low transpiration, similar to the findings of Yoshimura et al (2006) and Wen et al (2016).

As demonstrated by Phillips et al. (2003), Kocher et al. (2013), Čermák et al. (2007), and Urban et al. (2015), same-day RWU is the major contributor to daily transpiration of both coniferous and deciduous trees during the growing season in temperate and Mediterranean climates; whereas the tree-storage contribution during periods of low transpiration can be much larger (Hao et al., 2013). We anticipate that the simplification obtained by assuming ZS (and therefore EMMA methodologies for estimating RWU depths) would be most valid during periods of high transpiration and at locations with high soil water contents, whereas errors would grow at upslope locations and during periods of reduced soil water availability. The primary consideration for incorporating tree storage and mixing dynamics likely centers on the hydraulic storage capacity provided by the trees relative to the rate of RWU and transpiration. The choice of appropriate model structure is likely to be highly variable between hydroclimates and tree species.

Matheny et al. (2017) proposed that proper representation of plant dynamics could aid the parameterization of hydrologic models. Peaucelle et al. (2019) demonstrated that constraining an ecohydrological model with hydroclimatic observations yielded ecologically coherent model parameterizations. Mirfenderesgi et al. (2016) demonstrated that simulation of above ground tree water storage within hydrologic models improved estimates of stomatal conductance. Our conclusion is similar to these studies in that beech g_{smax} estimates derived within the WM and PF model structures were much closer to previously observed maximal stomatal conductances (Schäfer et al., 2000) than the calibrated values of the ZS model (Fig. 6). ZS, WM, and PF all yielded reasonable g_{smax} estimates for hemlock (Domec et al., 2013; Fig. 6). Improved model structures accounting for tree water storage will likely aid the incorporation of δ_{XYLEM} data in model parameter estimation efforts for ecohydrological and Earth system models.

4.3 Implications for Critical Zone Residence Times

Previous studies have estimated time lags between RWU and transpiration. Gaines et al. (2016) estimated growing season residence times of four deciduous tree species in Pennsylvania (approximately 200 km due south of our study catchment) as 5 to 22 days. In an artificial experimental mesocosm, Evaristo et al. (2019) estimated precipitation to transpiration transit times of tropical tree species of 17 to 62 days. Graefe et al. (2019) estimate residence times of five tree species in a dry forest ecosystem in Ecuador of 11 to 22 days. Within two coniferous species Meinzer et al. (2006) estimated residence times between 36 to 79 days. Our estimates of within-tree residence times were of similar order of magnitude to these studies. Accounting for the residence time within trees, as a component of the total critical zone residence time of transpired waters within this study catchment, increased estimates from 5% to 100% depending on tree species, season, and topographic position. This comparison broadly suggests distributed isotope-aided hydrologic models which explicitly simulate tree-dynamics may aid development of more complete estimates of critical zone residence times.

4.4 Ecohydrologic Modeling Framework

We simultaneously fit our model to several plot-scale observations (soil moisture content, δ_{SOILS}, and δ_{XYLEM}) as well as catchment-scale observations (stream discharge, δ_{STREAM}). The reproduction of the hydrologic cycle within the study period was reasonable (e.g. Fig. 2b; S4); however, some limitations must be discussed.

Across larger spatial scales, averaging over spatial heterogeneities has led to errors in the allocation of net land surface energy into latent heat fluxes, and further issues in partitioning latent heat losses between evaporation and transpiration (Rouholahnejad Freund et al., 2017; Chang et al., 2018). A 10 m horizontal grid resolution was selected to balance the spatial representation of water storage and fluxes with model computational demand. This horizontal grid, which averages over some topographic features, possibly led to some spurious results with respect to soil water content, δ_{SOILS}, and δ_{XYLEM}, which the MCMC algorithm attempted to fit. The greater abundance of plot scale measurements used for calibration (n = 820) likely overwhelmed the information content of the catchment-scale measurements (n = 538) in the GL function used for calibration (see Sect. 2.4) and led to a bias towards accurate reproduction of the plot-scale (Fig. S7a). Stronger reproduction of plot-scale fluxes possibly indicates issues of scale-dependence within this model as described in Clark et al. (2017). Relatively poorer

representation of catchment-scale water and isotopic fluxes could indicate the accumulation of grid-scale model structural errors as water propagated downstream across cells.

Several important simplifications within our sampling design and the model structure of EcH$_2$O-iso possibly influenced our conclusions. First, we assumed that extracted stem water was representative of mobile tree stored water in order to maintain a simplistic approach to the numerical representation of tree-stored water. As demonstrated by Zhao et al (2016) and De Deurwaerder et al (2019), there exists the possibility of isotopic variations within stems. Low variation in observed δ_{XYLEM} of both hemlock and beech at each location (Figures 3 and 4) suggested that this simplification was reasonable. Second, we assume that RWU is a non-fractionating process. Though some research has presented evidence for fractionation by RWU (e.g. Ellsworth and Williams, 2007; Vargas et al., 2017), this approach is common (Penna et al., 2018). Third, overestimation of the isotopic composition of spring and fall discharge (Fig. S4) was possibly attributable to the model assumption of complete percolate mixing (Kuppel et al., 2018a). Knighton et al (2019a) provided evidence for preferential recharge during snowmelt in the studied catchment, which would likely lead to a more depleted contribution of shallow groundwater to stream discharge. This could also be related to underestimation of the groundwater contribution. Future research on EcH$_2$O-iso may investigate the representation of snowpack accumulation and possible trade-offs between the simulation of plot-scale snow and catchment-scale discharge.

Finally, while EcH$_2$O-iso accounts for variability in RWU depth as water availability fluctuates within soil layers, the model incorporates the assumption that RWU depth-demand profiles, as defined by the K_{ROOT} parameter, are time-invariant throughout each simulation. Knighton et al. (2019a, b) and Mackay et al (2020) provided evidence that some coniferous trees shift RWU demand to deeper layers through periods of shallow soil water deficit. Recent studies have supported seasonal variations in RWU demand plasticity across a variety of tree species highlighting compensation mechanisms between wetter and water-limited layers (e.g. De Jong Van Lier et al. 2008; Javaux et al. 2008; Nehemy et al., 2019; Brinkmann et al., 2019). Brum et al (2019) and Knighton et al (2020) suggested that mixed species forests enhance RWU, possibly reflecting the development of complementary rooting strategies of forest stands. The assumption of a time-invariant RWU demand profile therefore likely contributed some structural uncertainty affecting RWU estimates that is difficult to assess with the sampling design of this study. Future research should incorporate more process-based ecohydrological simulation approaches that adequately reflect RWU responses to water limitation and vegetation root responses neighboring species.

5. Conclusions

Understanding the depth distribution of root water uptake (RWU) is critical to tracing water fluxes and ages through the critical zone. Despite the importance of plant roots in mediating stored soil water, relatively little is known about tree RWU. Recent studies involving stable water isotopic observations of soils and xylem waters as well as studies investigating tree water storage have challenged methodological assumptions within EMMA, particularly for water or energy limited settings with reduced transpiration (e.g., Penna et al., 2018).

We investigated the importance of tree water storage and internal mixing in the interpretation of δ_{XYLEM} for understanding the depth distribution of RWU and estimating critical zone water residence times. We performed a case study of the EcH$_2$O-iso model applied to a small

temperate catchment with a high density of both Eastern Hemlock (hemlock) and American Beech (beech). We modified EcH_2O-iso to simulate three cases: 1) no tree water storage (ZS; assuming δ_{RWU} is representative of δ_{XYLEM}, in line with the assumptions of EMMA), 2) well-mixed storage (WM; assuming trees are well mixed reservoirs) and 3) storage with piston flow (PF; assuming transpired water is always the oldest stored water). We fit each model structure to a set of hydrologic measurements, including three seasonal collections of hemlock and beech δ_{XYLEM} made across a hillslope, through a Markov-Chain Monte Carlo methodology.

The WM and PF models provided stronger agreement between simulated and observed summer and fall δ_{XYLEM} for both hemlock and beech than did the ZS case. The two approximations of internal tree-water mixing (WM and PF) yielded similar results for both beech and hemlock. Finally, we demonstrated that accounting for tree-storage residence times in both hemlock and beech increased estimates of critical zone residence times.

Our results suggest that there are likely to be advantages to considering tree storage and mixing when attempting to interpret δ_{XYLEM} in the estimation of RWU depths and critical zone water residence times, particularly during periods of low transpiration. Accounting for aboveground tree-water storage will likely improve how δ_{XYLEM} measurements can inform the ecohydrological models currently called for in the community (e.g. Penna et al., 2018), eventually yielding more accurate estimates of plant-water strategies in critical zone and Earth system models.

6. Data Availability

All study catchment hydrologic measurements are archived in the CUAHSI HydroClient database (https://data.cuahsi.org/) under the project CUISO (Knighton et al. 2019c). Hydrologic data may be accessed via the map application (latitude 42.42°, longitude -76.32°). The source code of the $EcH2O$-iso model used in this study is based on the branch master_KrootVeg available on the online repository https://bitbucket.org/sylka/ech2o_iso/. Post-processing tools to compute the above-ground tree water storage are available on the online repository https://github.com/jknigh0813/TreeStorageMixing.

7. Acknowledgements

8. References

Allen, S. T., Kirchner, J. W., Braun, S., Siegwolf, R. T., & Goldsmith, G. R. (2019). Seasonal origins of soil water used by trees. Hydrology and Earth System Sciences, 23(2), 1199-1210.

Barbeta, A., & Peñuelas, J. (2017). Relative contribution of groundwater to plant transpiration estimated with stable isotopes. Scientific reports, 7(1), 10580.

Barbeta, A., Ogée, J., & Peñuelas, J. (2018). Stable-Isotope Techniques to Investigate Sources of Plant Water. In Advances in Plant Ecophysiology Techniques (pp. 439-456). Springer, Cham.

Bartelink, H. H. (1997). Allometric relationships for biomass and leaf area of beech (Fagus sylvatica L). In Annales des sciences forestières (Vol. 54, No. 1, pp. 39-50). EDP Sciences.

Benettin, P., Queloz, P., Bensimon, M., McDonnell, J. J., & Rinaldo, A. (2019). Velocities, Residence Times, Tracer Breakthroughs in a Vegetated Lysimeter: A Multitracer Experiment. Water Resources Research, 55(1), 21-33.

Berry, Z. C., Evaristo, J., Moore, G., Poca, M., Steppe, K., Verrot, L., ... & Seyfried, M. (2018). The two water worlds hypothesis: Addressing multiple working hypotheses and proposing a way forward. Ecohydrology, 11(3), e1843.

Brantley, S. L., Eissenstat, D. M., Marshall, J. A., Godsey, S. E., Balogh-Brunstad, Z., Karwan, D. L., ... & Chadwick, O. (2017). Reviews and syntheses: on the roles trees play in building and plumbing the critical zone. Biogeosciences (Online), 14(22).

Braud, I., Bariac, T., Gaudet, J. P., & Vauclin, M. (2005). SiSPAT-Isotope, a coupled heat, water and stable isotope (HDO and H218O) transport model for bare soil. Part I. Model description and first verifications. Journal of Hydrology, 309(1-4), 277-300.

Brinkmann, N., Eugster, W., Buchmann, N., & Kahmen, A. (2019). Species-specific differences in water uptake depth of mature temperate trees vary with water availability in the soil. Plant Biology, 21(1), 71-81.

Brooks, J. R., Barnard, H. R., Coulombe, R., & McDonnell, J. J. (2010). Ecohydrologic separation of water between trees and streams in a Mediterranean climate. Nature Geoscience, 3(2), 100.

Brum, M., Vadeboncoeur, M. A., Ivanov, V., Asbjornsen, H., Saleska, S., Alves, L. F., et al. (2019). Hydrological niche segregation defines forest structure and drought tolerance strategies in a seasonal Amazon forest. Journal of Ecology, 107(1), 318–333. https://doi.org/10.1111/1365-2745.13022

Čermák, J., Kučera, J., Bauerle, W. L., Phillips, N., & Hinckley, T. M. (2007). Tree water storage and its diurnal dynamics related to sap flow and changes in stem volume in old-growth Douglas-fir trees. Tree physiology, 27(2), 181-198.

Chang, L. L., Dwivedi, R., Knowles, J. F., Fang, Y. H., Niu, G. Y., Pelletier, J. D., ... & Meixner, T. (2018). Why Do Large-Scale Land Surface Models Produce a Low Ratio

of Transpiration to Evapotranspiration?. Journal of Geophysical Research: Atmospheres, 123(17), 9109-9130.

Chitra-Tarak, R., Ruiz, L., Dattaraja, H. S., Mohan Kumar, M. S., Riotte, J., Suresh, H. S., ... & Sukumar, R. (2018). The roots of the drought: Hydrology and water uptake strategies mediate forest-wide demographic response to precipitation. Journal of Ecology, 106(4), 1495-1507.

Clark, M. P., Bierkens, M. F., Samaniego, L., Woods, R. A., Uijlenhoet, R., Bennett, K. E., ... & Peters-Lidard, C. D. (2017). The evolution of process-based hydrologic models: historical challenges and the collective quest for physical realism. Hydrology and Earth System Sciences (Online), 21(LA-UR-17-27603).

Comas, L. H., & Eissenstat, D. M. (2009). Patterns in root trait variation among 25 co-existing North American forest species. New Phytologist, 182(4), 919-928.

De Deurwaerder, H., Hervé-Fernández, P., Stahl, C., Burban, B., Petronelli, P., Hoffman, B., ... & Verbeeck, H. (2018). Liana and tree below-ground water competition—evidence for water resource partitioning during the dry season. Tree physiology, 38(7), 1071-1083.

De Deurwaerder, H., Visser, M. D., Detto, M., Boeckx, P., Meunier, F., Zhao, L., ... & Verbeeck, H. (2019). Diurnal variation in xylem water isotopic signature biases depth of root-water uptake estimates. bioRxiv, 712554.

De Jong van Lier, Q., Van Dam, J. C., Metselaar, K., De Jong, R., & Duijnisveld, W. H. M. (2008). Macroscopic root water uptake distribution using a matric flux potential approach. Vadose Zone Journal, 7(3), 1065-1078.

Domec, J. C., Rivera, L. N., King, J. S., Peszlen, I., Hain, F., Smith, B., & Frampton, J. (2013). Hemlock Woolly Adelgid (A delges tsugae) infestation affects water and carbon relations of Eastern Hemlock (T suga canadensis) and C arolina hemlock (T suga caroliniana). New Phytologist, 199(2), 452–463. https://doi.org/10.1111/nph.12263

Douinot, A. Tetzlaff, D. Maneta, M. Kuppel S. and Soulsby, C. (2019) Ecohydrological modelling with EcH2O-iso to quantify forest and grassland effects on water partitioning and flux ages. Hydrological Processes. DOI: 10.1002/hyp.13480.

Ellsworth, P. Z., & Williams, D. G. (2007). Hydrogen isotope fractionation during water uptake by woody xerophytes. Plant and Soil, 291(1-2), 93-107.

Evaristo, J., McDonnell, J. J., & Clemens, J. (2017). Plant source water apportionment using stable isotopes: A comparison of simple linear, two-compartment mixing model approaches. Hydrological processes, 31(21), 3750-3758.

Evaristo, J., & McDonnell, J. J. (2017). Prevalence and magnitude of groundwater use by vegetation: a global stable isotope meta-analysis. Scientific reports, 7, 44110.

Evaristo, J., Kim, M., van Haren, J., Pangle, L. A., Harman, C. J., Troch, P. A., & McDonnell, J. J. (2019). Characterizing the fluxes and age distribution of soil water, plant water, and deep percolation in a model tropical ecosystem. Water Resources Research.

Gaines, K. P., Meinzer, F. C., Duffy, C. J., Thomas, E. M., & Eissenstat, D. M. (2016). Rapid tree water transport and residence times in a Pennsylvania catchment. Ecohydrology, 9(8), 1554-1565.

Gee, G. W., and J. W. Bauder. 1986. Particle-size Analysis. P. 383 – 411. In A.L. Page (ed.). Methods of soil analysis, Part1, Physical and mineralogical methods. Second Edition, Agronomy Monograph 9, American Society of Agronomy, Madison, WI.

Goldsmith, G. R., Allen, S. T., Braun, S., Engbersen, N., González-Quijano, C. R., Kirchner, J. W., & Siegwolf, R. T. (2019). Spatial variation in throughfall, soil, and plant water isotopes in a temperate forest. Ecohydrology, 12(2), e2059.

Good, S. P., Noone, D., & Bowen, G. (2015). Hydrologic connectivity constrains partitioning of global terrestrial water fluxes. Science, 349(6244), 175-177.

Graefe, S., Fang, D., & Butz, P. Water residence times in trees of a neotropical dry forest. Trees, 1-7.

Hao, G. Y., Wheeler, J. K., Holbrook, N. M., & Goldstein, G. (2013). Investigating xylem embolism formation, refilling and water storage in tree trunks using frequency domain reflectometry. Journal of experimental botany, 64(8), 2321-2332.

Haverd, V., & Cuntz, M. (2010). Soil–Litter–Iso: A one-dimensional model for coupled transport of heat, water and stable isotopes in soil with a litter layer and root extraction. Journal of Hydrology, 388(3-4), 438-455.

Huo, G., Zhao, X., Gao, X., Wang, S., & Pan, Y. (2018). Seasonal water use patterns of rainfed jujube trees in stands of different ages under semiarid Plantations in China. Agriculture, ecosystems & environment, 265, 392-401.

Jackisch, C., Angermann, L., Allroggen, N., Sprenger, M., Blume, T., Tronicke, J., & Zehe, E. (2017). Form and function in hillslope hydrology: in situ imaging and characterization of flow-relevant structures. Hydrology and Earth System Sciences. DOI: 10.5194/hess-21-3749-2017

Javaux, M., Schröder, T., Vanderborght, J., & Vereecken, H. (2008). Use of a three-dimensional detailed modeling approach for predicting root water uptake. Vadose Zone Journal, 7(3), 1079-1088.

Kattge, J., Diaz, S., Lavorel, S., Prentice, I. C., Leadley, P., Bönisch, G., et al. (2011) TRY - a global database of plant traits. Global Change Biology 17:2905-2935.

Knighton, J., Saia, S. M., Morris, C. K., Archiblad, J. A., & Walter, M. T. (2017). Ecohydrologic considerations for modeling of stable water isotopes in a small intermittent watershed. Hydrological processes, 31(13), 2438-2452.

Knighton J., Souter-Kline, V., Volkmann, T., Troch, P., Kim, M., Harman, C., Morris, C., Buchanan, B., Walter, M.T. (2019a). Spatial and Topographic Variations in Ecohydrologic Separation in a Snow-Influenced Catchment. Water Resources Research. DOI:10.1029/2019WR025174

Knighton J., Coneelly, J., Walter, M. (2019b). Possible Increases in Flood Frequency Due to the Loss of Eastern Hemlock in the Northeastern US: Observational Insights and Predicted Impacts. Water Resources Research. DOI: 10.1029/2018WR024395

Knighton, J. (2019c). CUAHSI HIS: Cornell University Six Mile Creek Isotopes. DOI: 10.4211/his-5651

Knighton, J., Singh, K., & Evaristo, J. (2020). Understanding Catchment-Scale Forest Root Water Uptake Strategies Across the Continental United States Through Inverse Ecohydrological Modeling. Geophysical Research Letters, 47(1). DOI: 10.1029/2019GL085937

Köcher, P., Horna, V., Beckmeyer, I., & Leuschner, C. (2012). Hydraulic properties and embolism in small-diameter roots of five temperate broad-leaved tree species with contrasting drought tolerance. Annals of forest science, 69(6), 693-703.

Kravka, M., Krejzar, T., & Čermák, J. (1999). Water content in stem wood of large pine and spruce trees in natural forests in central Sweden. Agricultural and Forest Meteorology, 98, 555-562.

Kuppel, S., Tetzlaff, D., Maneta, M., & Soulsby, C. (2018a). EcH$_2$O-iso 1.0: water isotopes and age tracking in a process-based, distributed ecohydrological model. Geoscientific Model Development, 11, 3045-3069. DOI: 10.5194/gmd-11-3045-2018

Kuppel, S., Tetzlaff, D., Maneta, M. P., & Soulsby, C. (2018b). What can we learn from multi-data calibration of a process-based ecohydrological model?. Environmental Modelling & Software, 101, 301-316.

Leuschner, C., Voß, S., Foetzki, A., & Clases, Y. (2006). Variation in leaf area index and stand leaf mass of European beech across gradients of soil acidity and precipitation. Plant Ecology, 186(2), 247-258.

Mackay, D. S., Savoy, P. R., Grossiord, C., Tai, X., Pleban, J. R., Wang, D. R., ... & Sperry, J. S. (2020). Conifers depend on established roots during drought: results from a coupled model of carbon allocation and hydraulics. New Phytologist, 225(2), 679-692.

Maneta, M. P., & Silverman, N. L. (2013). A spatially distributed model to simulate water, energy, and vegetation dynamics using information from regional climate models. Earth Interactions, 17(11), 1-44.

Matheny, A. M., Mirfenderesgi, G., & Bohrer, G. (2017). Trait-based representation of hydrological functional properties of plants in weather and ecosystem models. Plant diversity, 39(1), 1-12.

Matheny, A. M., Bohrer, G., Garrity, S. R., Morin, T. H., Howard, C. J., & Vogel, C. S. (2015). Observations of stem water storage in trees of opposing hydraulic strategies. Ecosphere, 6(9), 1-13.

McCutcheon, R. J., McNamara, J. P., Kohn, M. J., & Evans, S. L. (2017). An evaluation of the ecohydrological separation hypothesis in a semiarid catchment. Hydrological processes, 31(4), 783-799.

Meinzer, F. C., Woodruff, D. R., Eissenstat, D. M., Lin, H. S., Adams, T. S., & McCulloh, K. A. (2013). Above-and belowground controls on water use by trees of different wood types in an eastern US deciduous forest. Tree physiology, 33(4), 345-356.

Meinzer, F. C., Brooks, J. R., Domec, J. C., Gartner, B. L., Warren, J. M., Woodruff, D. R., ... & Shaw, D. C. (2006). Dynamics of water transport and storage in conifers studied with deuterium and heat tracing techniques. Plant, Cell & Environment, 29(1), 105-114.

Mirfenderesgi, G., Bohrer, G., Matheny, A. M., Fatichi, S., de Moraes Frasson, R. P., & Schäfer, K. V. (2016). Tree level hydrodynamic approach for resolving aboveground water storage and stomatal conductance and modeling the effects of tree hydraulic strategy. Journal of Geophysical Research: Biogeosciences, 121(7), 1792-1813.

Naithani, K. J., Baldwin, D. C., Gaines, K. P., Lin, H., & Eissenstat, D. M. (2013). Spatial distribution of tree species governs the spatio-temporal interaction of leaf area index and soil moisture across a forested landscape. PLoS One, 8(3), e58704.

Nehemy, M. F., Benettin, P., Asadollahi, M., Pratt, D., Rinaldo, A., & McDonnell, J. J. (2019). How plant water status drives tree source water partitioning. Hydrology and Earth System Sciences: Discussions. DOI: 10.5194/hess-2019-528

Northeast Regional Climate Center (NRCC). (2019). The Ithaca Climate Page. Available Online: http://www.nrcc.cornell.edu/wxstation/ithaca/ithaca.html. Accessed on: 6/20/2019

Natural Resources Conservation Service (NRCS), United States Department of Agriculture. (2019).Web Soil Survey. Available online at the following link: https://websoilsurvey.sc.egov.usda.gov/. Accessed on: 5/2/2019.

Peaucelle, M., Bacour, C., Ciais, P., Vuichard, N., Kuppel, S., Peñuelas, J., ... & Delpierre, N. (2019). Covariations between plant functional traits emerge from constraining parameterization of a terrestrial biosphere model. Global Ecology and Biogeography, 28(9), 1351-1365.

Penna, D., Hopp, L., Scandellari, F., Allen, S. T., Benettin, P., Beyer, M., ... & Volkmann, T. (2018). Ideas and perspectives: Tracing terrestrial ecosystem water fluxes using hydrogen and oxygen stable isotopes–challenges and opportunities from an interdisciplinary perspective. Biogeosciences. DOI: 10.5194/bg-15-6399-2018

Pfautsch, S., Renard, J., Tjoelker, M. G., & Salih, A. (2015). Phloem as capacitor: radial transfer of water into xylem of tree stems occurs via symplastic transport in ray parenchyma. Plant Physiology, 167(3), 963-971.

Phillips, N. G., Ryan, M. G., Bond, B. J., McDowell, N. G., Hinckley, T. M., & Čermák, J. (2003). Reliance on stored water increases with tree size in three species in the Pacific Northwest. Tree Physiology, 23(4), 237-245.

Rothfuss, Y., & Javaux, M. (2017). Reviews and syntheses: Isotopic approaches to quantify root water uptake: a review and comparison of methods. Biogeosciences, 14, 2199.

Rouholahnejad Freund, E., & Kirchner, J. W. (2017). A Budyko framework for estimating how spatial heterogeneity and lateral moisture redistribution affect average

evapotranspiration rates as seen from the atmosphere. Hydrology and Earth System Sciences, 21(1), 217-233.

Sanchez-Costa, E., Poyatos, R., & Sabate, S. (2015). Contrasting growth and water use strategies in four co-occurring Mediterranean tree species revealed by concurrent measurements of sap flow and stem diameter variations. Agricultural and Forest Meteorology, 207, 24-37.

Schäfer, K. V. R., Oren, R., & Tenhunen, J. D. (2000). The effect of tree height on crown level stomatal conductance. Plant, Cell & Environment, 23(4), 365–375. https://doi.org/10.1046/j.1365-3040.2000.00553.x

Schlesinger, W. H., & Jasechko, S. (2014). Transpiration in the global water cycle. Agricultural and Forest Meteorology, 189, 115-117.

Schneiderman, E. M., Steenhuis, T. S., Thongs, D. J., Easton, Z. M., Zion, M. S., Neal, A. L., ... & Todd Walter, M. (2007). Incorporating variable source area hydrology into a curve-number-based watershed model. Hydrological Processes: An International Journal, 21(25), 3420-3430.

Scholz, F. G., Phillips, N. G., Bucci, S. J., Meinzer, F. C., & Goldstein, G. (2011). Hydraulic capacitance: biophysics and functional significance of internal water sources in relation to tree size. In Size-and age-related changes in tree structure and function (pp. 341-361). Springer, Dordrecht.

Schoups, G., & Vrugt, J. A. (2010). A formal likelihood function for parameter and predictive inference of hydrologic models with correlated, heteroscedastic, and non-Gaussian errors. Water Resources Research, 46(10).

Smith, A., Welch, C., & Stadnyk, T. (2016). Assessment of a lumped coupled flow-isotope model in data scarce Boreal catchments. Hydrological Processes, 30(21), 3871-3884.

Smith, A. A. (In Review). Using StorAge Selection functions to quantify ecohydrological controls on the time-variant age of evapotranspiration, soil water, and recharge. Advances in Water Resources.

Sprenger, M., Tetzlaff, D., Buttle, J., Carey, S. K., McNamara, J. P., Laudon, H., ... & Soulsby, C. (2018). Storage, mixing, and fluxes of water in the critical zone across northern environments inferred by stable isotopes of soil water. Hydrological processes, 32(12), 1720-1737.

Sprenger, M., Stumpp, C., Weiler, M., Aeschbach, W., Allen, S. T., Benettin, P., ... & McDonnell, J. J. (2019). The demographics of water: A review of water ages in the critical zone. Reviews of Geophysics.

Staelens, J., De Schrijver, A., Verheyen, K., & Verhoest, N. E. (2006). Spatial variability and temporal stability of throughfall water under a dominant beech (Fagus sylvatica L.) tree in relationship to canopy cover. Journal of hydrology, 330(3-4), 651-662.

Treydte, K., Boda, S., Graf Pannatier, E., Fonti, P., Frank, D., Ullrich, B., ... & Gessler, A. (2014). Seasonal transfer of oxygen isotopes from precipitation and soil to the tree ring: source water versus needle water enrichment. New Phytologist, 202(3), 772-783.

Urban, J., Čermák, J., & Ceulemans, R. (2015). Above-and below-ground biomass, surface and volume, and stored water in a mature Scots pine stand. European journal of forest research, 134(1), 61-74.

Vargas, A. I., Schaffer, B., Yuhong, L., & Sternberg, L. D. S. L. (2017). Testing plant use of mobile vs immobile soil water sources using stable isotope experiments. New Phytologist, 215(2), 582-594.

Volkmann, T. H., Haberer, K., Gessler, A., & Weiler, M. (2016). High-resolution isotope measurements resolve rapid ecohydrological dynamics at the soil–plant interface. New Phytologist, 210(3), 839-849.

Wang, J., Fu, B., Lu, N., & Zhang, L. (2017). Seasonal variation in water uptake patterns of three plant species based on stable isotopes in the semi-arid Loess Plateau. Science of the Total Environment, 609, 27-37.

Wang, J., Fu, B., Lu, N., Wang, S., & Zhang, L. (2019). Water use characteristics of native and exotic shrub species in the semi-arid Loess Plateau using an isotope technique. Agriculture, Ecosystems & Environment, 276, 55-63.

Wen, X., Yang, B., Sun, X., & Lee, X. (2016). Evapotranspiration partitioning through in-situ oxygen isotope measurements in an oasis cropland. Agricultural and Forest Meteorology, 230, 89-96.

Yanai, R. D., Fisk, M. C., Fahey, T. J., Cleavitt, N. L., & Park, B. B. (2008). Identifying roots of northern hardwood species: patterns with diameter and depth. Canadian Journal of Forest Research, 38(11), 2862-2869.

Yoshimura, K., Miyazaki, S., Kanae, S., & Oki, T. (2006). Iso-MATSIRO, a land surface model that incorporates stable water isotopes. Global and Planetary Change, 51(1-2), 90-107.

Zhao, L., Wang, L., Cernusak, L. A., Liu, X., Xiao, H., Zhou, M., & Zhang, S. (2016). Significant difference in hydrogen isotope composition between xylem and tissue water in Populus euphratica. Plant, cell & environment, 39(8), 1848-1857.

Zimmermann MH (1971) Storage, mobilization and circulation of assimilates. In: Zimmermann MH, Brown CL (eds) Trees, structure and function. Springer, Berlin Heidelberg New York, pp 307–319
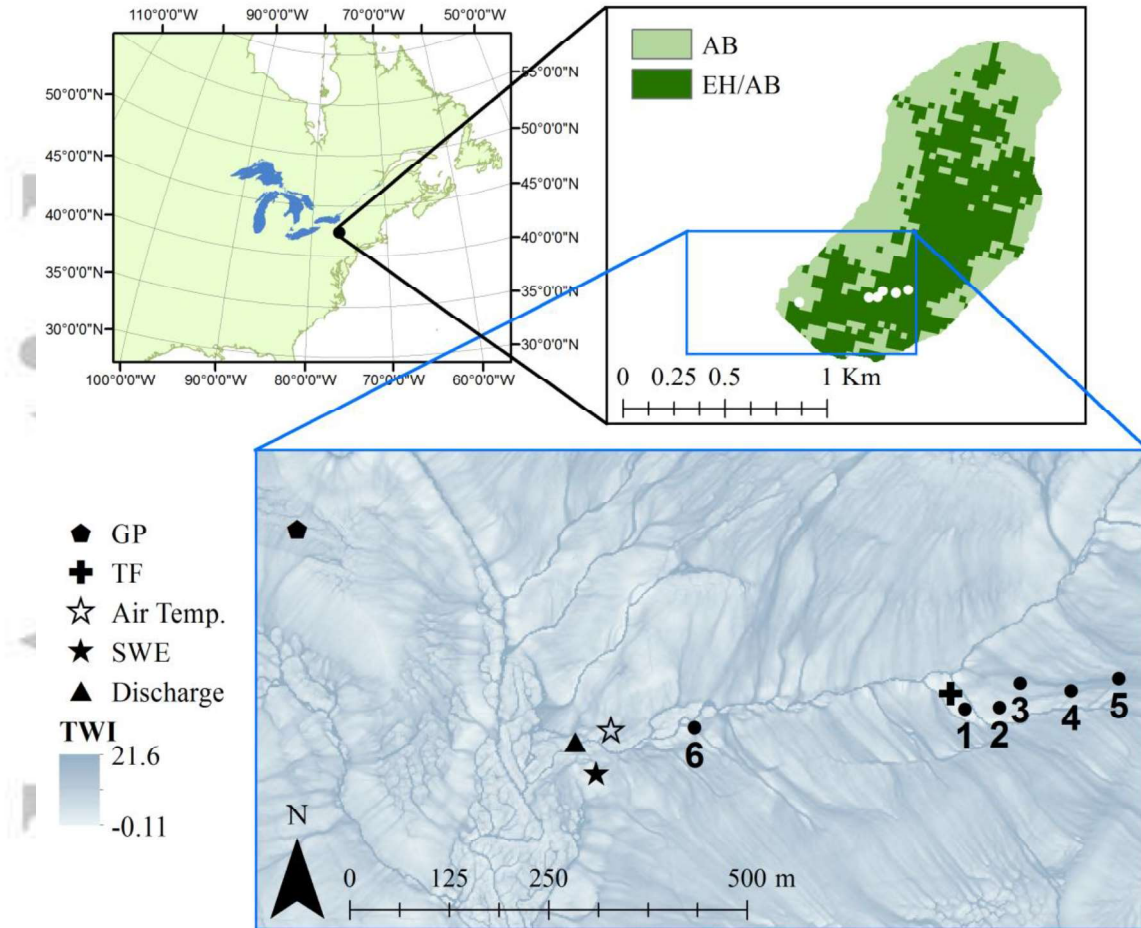
*Fig. 1 – Study catchment plant composition and sampling locations (black circles). TF –
throughfall, SWE – snow water equivalent, TWI – topographic wetness index. The six soil
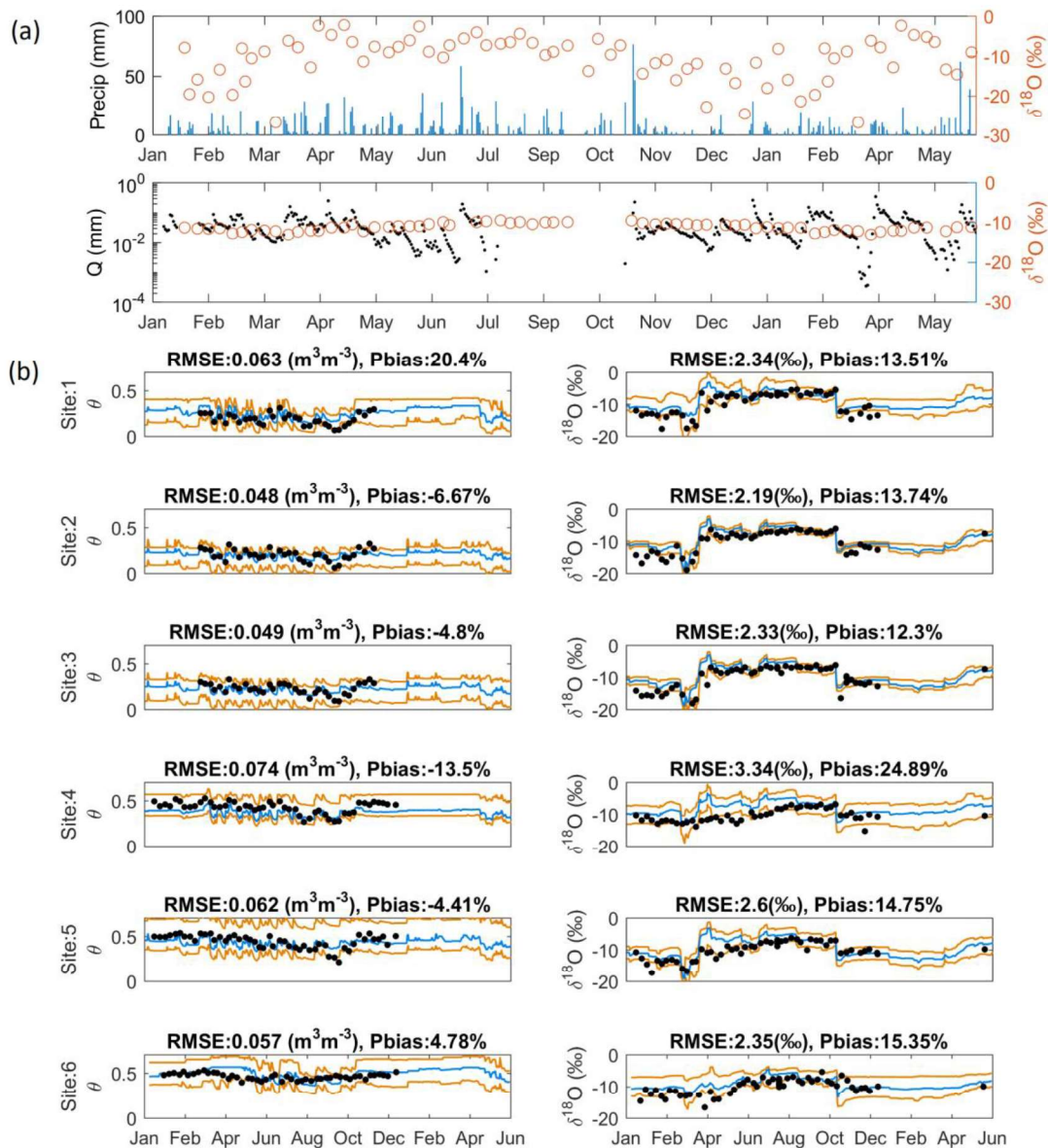sampling locations (numbered) correspond to Fig. 1.*

Fig. 2 – Time series of a) precipitation, catchment discharge and isotopic composition, and b) Zero Storage (ZS) case calibration results for soil Volumetric Water Content (Ɵ) and soil isotopic composition (δSOILS) of the upper (10 cm) soil layer (median – blue, 90% prediction interval – orange)
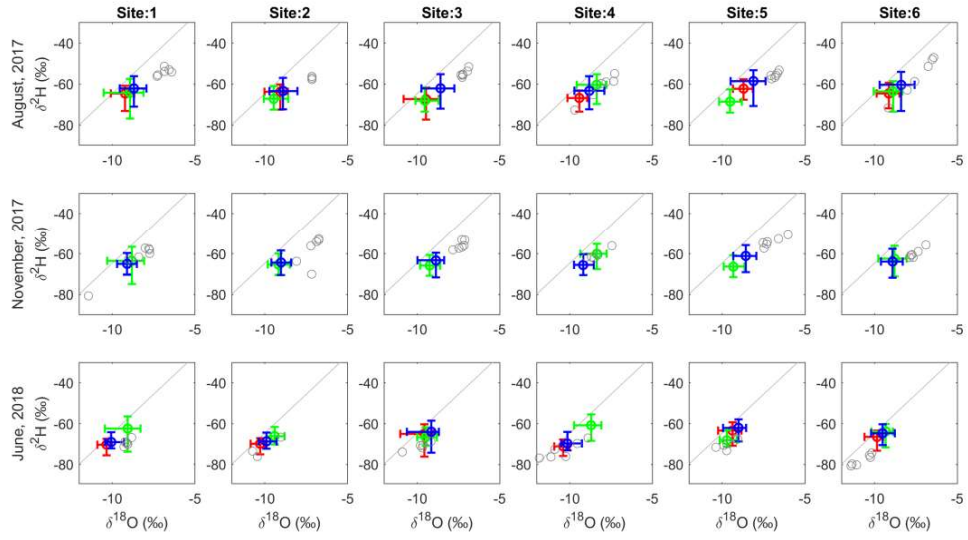
Fig. 3 – American Beech dual isotope space comparison of ZS (red), WM (green) and PF (blue), and observed soils across all depths (gray). Error bars represent the 5ᵗʰ and 95ᵗʰ percentiles of accepted model parameter simulations (or observations in the case of soils). Open circles are observed xylem. ZS does not appear November, 2017, as simulated beech was not taking up soil water at that time.
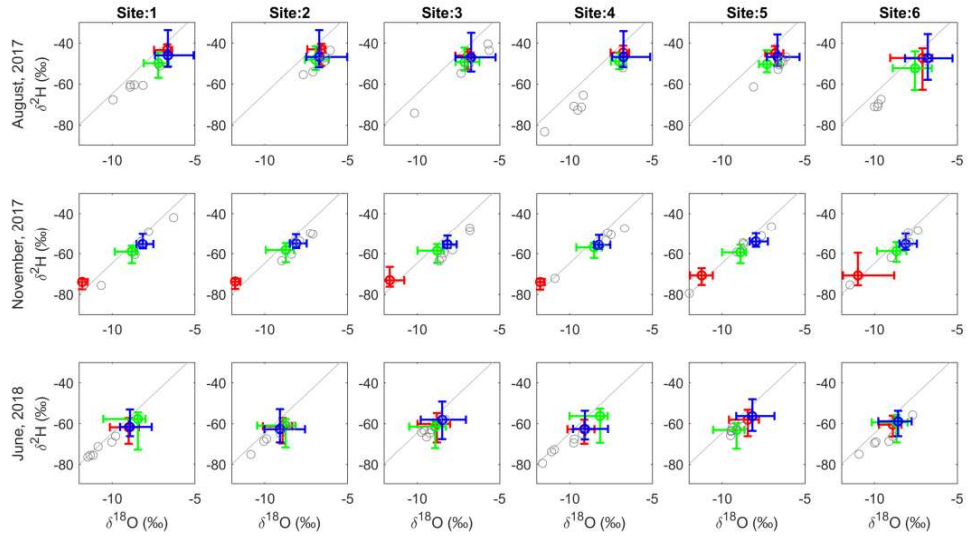
Fig. 4 – Eastern hemlock dual isotope space comparison of ZS (red), WM (green) and PF (blue). Error bars represent the 5th and 95th percentiles of accepted model simulations. Open circles are observed xylem.

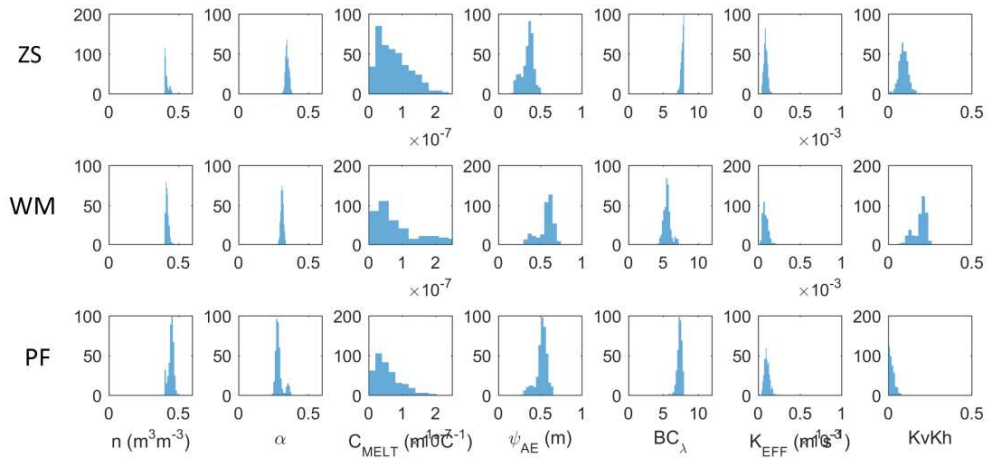*Fig. 5 – Posterior distributions of EcH₂O-iso hydrologic parameters*

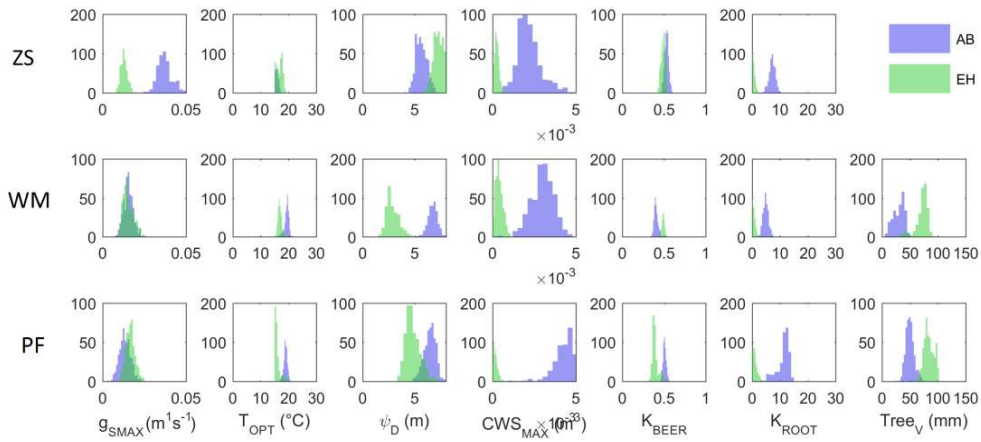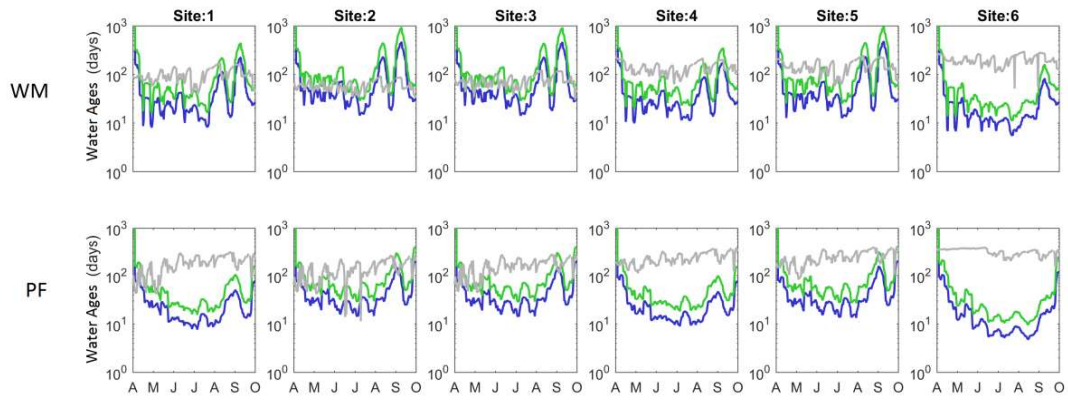*Fig. 6 – Posterior parameter distributions for plant dynamics parameters for Eastern Hemlock (green) and American Beech (purple)*

Fig. 7 – Simulated one week moving average of the age of RWU (gray) and residence times in both hemlock (green) and beech (blue) tree storage within the WM and PF model structures from April through October 2017

*Table1 – Properties of soil and plant sampling locations. Soil properties are representative of the top 30 cm. Plant densities were measured within a 6 m radius around the soil sampling location. * beech individuals existed just beyond the 6 m radius.*

Location	TWI	Sand (%)	Clay (%)	Beech (m^{-2})	Hemlock (m^{-2})
1	1.45	66	11	0.013	0.034
2	3.58	66	12	0*	0.04
3	5.5	77	11	0.013	0.027
4	8.4	71	12	0.014	0.034
5	10.2	76	8	0.02	0.027
6	12.48	76	5	0.02	0.027

Table 2 – Observed data and residuals used for model calibration

	Residual Metric	Field Locations	Model Compartment	Time Interval
Discharge	mm^{1}day^{-1}, δ^{18}O (‰)	Outlet	Outlet	Daily
Snowpack	SWE (mm)	SWE (pixel)	SWE (pixel)	Weekly
Soil Water (top 10 cm)	VWC (%)	2, 5	Upper 10 cm (pixel)	Weekly
Bulk δ_{SOILS} (top 10 cm)	δ^{18}O (‰)	2, 5	Upper 10 cm (pixel)	Weekly
Beech xylem water	d-excess (‰), MWL (‰)	1, 2, 3, 4, 5, 6	NS, WM, PF (pixel)	Seasonal
Hemlock xylem water	d-excess (‰), MWL (‰)	1, 2, 3, 4, 5, 6	NS, WM, PF (pixel)	Seasonal

Table 3 – EcH₂O-iso parameters used for model calibration. Plant parameters were fit for both hemlock and beech.

Parameter	Module	Description	Units	Range
n	hydrologic	soil porosity	$m^3 m^{-3}$	(0.3, 0.6)
α	hydrologic	albedo	-	(0, 1)
C_{MELT}	hydrologic	snowmelt coef.	$m^1 s^{-1} °C^{-1}$	(0, 3e7)
ψ_{AE}	hydrologic	air entry pressure head	m	(0, 1)
BC_λ	hydrologic	Brooks Corey exponent	-	(0, 12)
K_{EFF}	hydrologic	saturated horizontal soil conductivity	$m^1 s^{-1}$	(0, 1e-3)
KvKh	hydrologic	ratio of vertical to horiz. K_{EFF}	-	(0, 1)
g_{Smax}	plant	maximum stomatal conductance	$m^1 s^{-1}$	(0, 0.05)
T_{OPT}	plant	optimal growth temperature	°C	(0, 30)
ψ_D	plant	soil water potential halving stomatal conductance	m	(0, 8)
CWS_{max}	plant	maximum canopy water storage	$m^1 LAI^{-1}$	(0, 5e-3)
K_{BEER}	plant	light extinction coefficient	-	(0, 1)
K_{ROOT}	plant	RWU profile	m^{-1}	(0, 30)
$Tree_V$	plant	tree storage volume of mobile water	mm	(0, 150)

Table 4 – Zero storage (ZS), Well mixed (WM), and Piston flow (PF) residuals for d-excess and MWL for hemlock and beech.
** Indicates best performance by species and season

		Eastern Hemlock						American Beech					
		D-Excess Residual (‰)			MWL Residual (‰)			D-Excess Residual (‰)			MWL Residual (‰)		
Season	Site	ZS	WM	PF	ZS	WM	PF	ZS	WM	PF	ZS	WM	PF
Summer	1	1.3	0.8	0.5	22.5	10.5	6.6	6.4	7.0	7.2	16.2	5.1	6.5
	2	6.3	4.2	4.4	14.1	4.3	5.5	7.8	7.7	8.1	10.0	13.3	8.6
	3	5.5	3.4	3.0	16.5	6.3	4.3	5.4	5.2	5.2	12.8	10.5	3.8
	4	4.2	1.8	2.8	31.5	17.6	14.3	3.4	3.9	4.9	2.8	11.5	13.0
	5	8.1	6.0	5.3	15.4	4.7	0.0	9.0	9.0	8.6	13.1	10.6	8.9
	6	1.6	1.3	0.5	27.1	2.1	11.6	5.0	4.9	5.2	9.3	10.5	7.7
Average		**4.5**	**2.9**	**2.7****	**21.2**	**7.6**	**7.1****	**6.2****	**6.3**	**6.5**	**10.7**	**10.2**	**8.1****
Fall	1	8.2	1.8	2.1	9.9	2.0	1.2	-	3.4	3.0	-	3.2	6.7
	2	12.1	2.4	1.2	15.4	3.2	2.5	-	10.8	10.3	-	7.2	2.6
	3	14.2	4.6	2.8	14.3	3.7	2.1	-	6.5	5.4	-	3.9	0.4
	4	8.6	0.7	0.6	13.4	4.3	4.0	-	2.3	2.5	-	0.5	4.1
	5	7.1	2.4	4.4	13.0	3.7	3.1	-	7.7	6.3	-	0.4	0.9
	6	5.8	4.5	2.7	10.5	9.6	1.7	-	7.1	8.2	-	7.1	3.0
Average		**9.3**	**2.7**	**2.3****	**12.7**	**4.4**	**2.4****	**-**	**6.3**	**5.9****	**-**	**3.7**	**2.9****
Spring	1	4.9	6.0	2.6	16.4	9.5	9.4	7.6	4.5	7.2	2.0	6.9	7.4
	2	0.6	0.6	2.0	10.1	1.2	2.0	3.4	0.8	2.4	0.4	14.3	8.9
	3	1.7	0.6	0.3	6.8	2.5	3.4	4.3	1.8	3.0	0.8	12.6	12.0
	4	3.3	3.9	0.5	18.1	8.6	8.0	0.5	2.3	0.6	8.6	11.6	10.7
	5	2.1	1.1	0.6	5.8	3.0	5.4	4.5	2.2	2.8	2.4	9.4	13.2
	6	1.3	1.0	3.2	11.6	1.1	6.3	3.7	0.9	2.6	10.5	12.2	17.7
Average		**2.3**	**2.2**	**1.5****	**11.4**	**4.3****	**5.7**	**4.0**	**2.1****	**3.1**	**4.1****	**11.1**	**11.6**